JHEP

Published for SISSA by Springer

Received: February 28, 2014
Accepted: May 15, 2014
Published: June 12, 2014

Benchmarks for dark matter searches at the LHC

Andrea De Simone,[a] **Gian Francesco Giudice**[b,c] **and Alessandro Strumia**[d,e]

[a] *SISSA and INFN, Sezione di Trieste, via Bonomea 265, I-34136 Trieste, Italy*
[b] *CERN, Theory Division, CH-1211 Geneva 23, Switzerland*
[c] *Solvay Institute, Boulevard du Triomphe, 1050 Bruxelles, Belgium*
[d] *Dipartimento di Fisica dell'Università di Pisa and INFN, Italy*
[e] *National Institute of Chemical Physics and Biophysics, Tallinn, Estonia*

E-mail: andrea.desimone@sissa.it, gian.giudice@cern.ch, astrumia@mail.df.unipi.it

Abstract: We propose some scenarios to pursue dark matter searches at the LHC in a fairly model-independent way. The first benchmark case is dark matter co-annihilations with coloured particles (gluinos or squarks being special examples). We determine the masses that lead to the correct thermal relic density including, for the first time, strong Sommerfeld corrections taking into account colour decomposition. In the second benchmark case we consider dark matter that couples to SM particles via the Z or the Higgs. We determine the couplings allowed by present experiments and discuss future prospects. Finally we present the case of dark matter that freezes out via decays and apply our results to invisible Z and Higgs decays.

Keywords: Beyond Standard Model, Cosmology of Theories beyond the SM

ArXiv ePrint: 1402.6287

doi:10.1007/JHEP06(2014)081

JHEP06(2014)081

Contents

1 Introduction

The traditional search for Dark Matter (DM) at the LHC is based on specific theoretical models that are motivated by solving the naturalness problem. Supersymmetry is the prototypical example. The lack of evidence for new physics in the first phase of the LHC, together with the negative results from direct and indirect searches of galactic halo DM, have cast some doubts on the paradigm linking DM to natural electroweak (EW) theories. This has motivated new and more model-independent strategies for DM searches at colliders, and led to a vast literature on the subject [1–88].

A common approach used to describe the unknown interactions between DM and SM particles is resorting to a set of effective operators [3–5, 7–10, 13, 14, 16, 20, 23, 28, 30, 35, 36, 39, 40, 42–46, 48, 50, 62, 88]. An example is a four-fermion interaction between a spin-1/2 DM particle (χ) and quarks of the kind $(\bar{q}\gamma_\mu q)(\chi\gamma^\mu\chi)/\Lambda^2$, where Λ is an effective energy scale. At first sight, this approach appears to be fully model-independent, although in practice it has limited validity [24, 26, 49, 51, 57, 64]. At the LHC, the signature is missing energy (from DM) accompanied by a single jet, photon, or Z (required for tagging the event). The signal rate, after the cuts necessary to reduce the SM background, is rather small. This implies that the scales Λ of the effective operators probed by the LHC are often smaller than the energy of the partons involved in the collision ($\sqrt{\hat{s}}$), thus invalidating the use of an effective field theory. As a result, the interpretation of LHC data in terms of effective operators can lead to erroneous conclusions. It can deceptively

JHEP06(2014)081

overestimate the DM signal, because of spurious enhancements proportional to powers of $\sqrt{\hat{s}}/\Lambda$. Or it can underestimate the actual reach of the LHC search, when the particle that mediates the effective operator is within the kinematical range and gives a much better collider signal than the "model-independent" DM particle production. Also, the effective-operator approach leads to LHC bounds on the cross sections relevant for direct DM detection that seem very competitive, but are often only illusory. While the effective-operator approximation can be trusted for the low momentum transfers involved in direct detection, an operator with large dimensionality can misleadingly reward LHC for its high energy.

An alternative approach is to classify possible mediators of the interactions between DM and SM particles [6, 19, 22, 24, 29, 32, 34, 38, 41, 52–56, 87]. One class of mediators is given by particles exchanged in the s-channel of the DM annihilation process (or, inversely, in the DM production process at colliders). These mediators must be electrically neutral and can have spin 0 or 1. The most popular example is a new vector boson Z'. A second class of mediators consists of particles exchanged in the t-channel. An interesting possibility for the LHC is that the dominant DM annihilation channel is into a quark-antiquark pair and that the t-channel mediator is a colour triplet, which is a scalar or vector (if DM has spin 1/2) or a spinor (if DM has spin 0). Direct DM searches give strong constraints on the mediator interactions, but there are still certain windows of mediator mass and couplings that lead to a correct thermal relic abundance and that can be explored by future LHC runs.

The importance of the hunt for DM and our ignorance of its nature entail that the LHC must pursue a diversified, complete, and model-independent program searching for DM. With this paper, we want to contribute to the subject by proposing alternative approaches for strategies that experiments at the LHC can follow in the investigation of DM. In section 2, we consider a situation in which the DM thermal relic abundance is determined by co-annihilation with a coloured particle. In section 3, we study the case in which the DM abundance is determined by the coupling with the Z or Higgs boson. In section 4 we analyse the case in which the DM abundance is determined by thermal freeze-out of decays, and apply our results to invisible Z and Higgs decays. Finally, section 5 contains a summary of our results.

2 DM co-annihilating with a coloured partner

We consider the possibility that the DM particle, stabilized by a discrete symmetry, is accompanied by a nearby coloured state χ', either in the triplet or octet representation of $\mathrm{SU}(3)_c$, which can be either a scalar or a fermion. These four situations are summarised in the following table:

χ'	Colour triplet	Colour octet
Scalar	S3	S8
Fermion	F3	F8

JHEP06(2014)081

Since we neglect any interaction between the SM and dark sectors, other than strong interactions, there are only two parameters relevant for our analysis: the DM mass $M_{\rm DM}$ and the mass splitting ΔM of χ' with respect to the DM.

2.1 DM relic density

The relic abundance follows from the standard freeze-out mechanism described by the Boltzmann equation for the total number density of the dark system normalised to the entropy density $Y = n/s$, as a function of $z = M_{\rm DM}/T$

$$\frac{{\rm d}Y}{{\rm d}z} = -f(z)(Y^2 - Y_{\rm eq}^2)\,, \tag{2.1}$$

where $Y_{\rm eq}$ is the thermal equilibrium value of Y and

$$f(z) \equiv \left(1 + \frac{1}{3}\frac{{\rm d}\ln g_{*S}}{{\rm d}\ln T}\right)\frac{s\langle\sigma v\rangle}{zH} \approx \frac{1}{z^2}\sqrt{\frac{\pi g_*}{45}}M_{\rm Pl}M_{\rm DM}\langle\sigma v\rangle\,, \tag{2.2}$$

g_* (g_{*S}) being the number of degrees of freedom that describes the total energy (entropy) of the thermal system. As well known, by solving the Boltzmann equations one finds that the observed DM abundance is reproduced for

$$\langle\sigma v\rangle_{\rm cosmo} = (2.3 \pm 0.1) \times 10^{-26}\,{\rm cm}^3\,{\rm s}^{-1} \tag{2.3}$$

at $T \approx M_{\rm DM}/25$. In the following we give explicit results for $\langle\sigma v\rangle$ keeping only the dominant s-wave annihilations, while subleading p-wave annihilations are included in our numerical final result.

The dark system is composed by the DM particle χ, which negligibly annihilates, and by the coloured partner χ' which efficiently self-annihilates via QCD interactions. The two dark particles are kept in thermal equilibrium among themselves by dark interactions. The same interactions will be responsible for the decay of χ' into χ. We assume for simplicity that one χ particle is produced in each χ' decay. One can describe this system by a single Boltzmann equation of the form (2.1) for the quantity $Y = g_\chi Y_\chi + g_{\chi'}Y_{\chi'}$, and effective cross section

$$\langle\sigma v\rangle = \sigma(\chi'\chi' \to \text{SM particles})v \times R^2, \tag{2.4}$$

where

$$R = \frac{g_{\chi'}Y_{\chi'}^{\rm eq}}{g_\chi Y_\chi^{\rm eq} + g_{\chi'}Y_{\chi'}^{\rm eq}} = \left[1 + \frac{g_\chi}{g_{\chi'}}\frac{\exp(\Delta M/T)}{(1+\Delta M/M_{\rm DM})^{3/2}}\right]^{-1}\,. \tag{2.5}$$

The annihilation channels for the self-conjugate colour octet and for the colour triplet-antitriplet pair are two gluons (gg) and SM quarks ($q\bar{q}$). The number of degrees of freedom is $g_{\chi'} = \{6, 8, 12, 16\}$ for {S3, S8, F3, F8} respectively. In terms of the quadratic Casimir invariant $C(R)$ and the Dynkin index $T(R)$ of a generic irreducible representation R with generators T^a,

$$\delta_{ij}C(R) = (T^aT^a)_{ij}\,, \qquad \delta^{ab}T(R) = {\rm Tr}(T^aT^b)\,, \tag{2.6}$$

JHEP06(2014)081

we can express the quartic invariants as

$$K_1(R) \equiv \mathrm{Tr}(T^a T^a T^b T^b) = d(R) C^2(R) \tag{2.7}$$

$$K_2(R) \equiv \mathrm{Tr}(T^a T^b T^a T^b) = K_1(R) - \frac{d(A) C(A) T(R)}{2} \,. \tag{2.8}$$

Here $d(R)$ is the dimensionality of the irreducible representation R, and A refers to the adjoint representation. For the fundamental and adjoint of SU(N), one has

R	d	T	C	K_1	K_2
fundamental	N	$\frac{1}{2}$	$\frac{N^2-1}{2N}$	$\frac{(N^2-1)^2}{4N}$	$-\frac{N^2-1}{4N}$
adjoint	N^2-1	N	N	$N^2(N^2-1)$	$\frac{N^2(N^2-1)}{2}$

. (2.9)

Thus, in the case of interest, we find

χ'	d	T	C	K_1	K_2
S3, F3	3	$\frac{1}{2}$	$\frac{4}{3}$	$\frac{16}{3}$	$-\frac{2}{3}$
S8, F8	8	3	3	72	36

. (2.10)

In the non-relativistic limit, the annihilation cross sections into gluons is given by[1]

$$\sigma(\chi'\chi' \to gg) v = \frac{(K_1 + K_2)}{16\pi g_{\chi'} d} \frac{g_3^4}{M_{\chi'}^2} \,, \tag{2.11}$$

where g_3 is the QCD coupling and $M_{\chi'}$ is the mass of χ'. The annihilation cross section into the six SM quarks (taken to be massless) is

$$\sigma(\chi'\chi' \to q\bar{q}) v = \frac{3T(R)}{\pi g_{\chi'} d} \frac{g_3^4}{M_{\chi'}^2} \times \begin{cases} 1 \text{ if } \chi' \text{ is a fermion} \\ 0 \text{ if } \chi' \text{ is a boson} \end{cases} \,. \tag{2.12}$$

We neglected the electroweak contributions to the annihilation cross sections with respect to the dominant QCD effects. If χ' is a scalar (S3, S8), its annihilations into fermions are p-wave suppressed.

Summarising, in the four cases of interest, the total χ' annihilation cross sections are

$$\sigma(\chi'\chi' \to gg, q\bar{q}) v = \frac{g_3^4}{M_{\chi'}^2} \times \begin{cases} \frac{7}{432\pi} & \text{(scalar triplet)} \\ \frac{27}{256\pi} & \text{(scalar octet)} \\ \frac{7}{864\pi} + \frac{1}{24\pi} & \text{(fermion triplet)} \\ \frac{27}{512\pi} + \frac{9}{128\pi} & \text{(fermion octet)} \end{cases} \,, \tag{2.13}$$

where we have kept separated the contributions from annihilations into gluons and quarks. The nature of the DM particle enters only in the factor R of eq. (2.5). If $\Delta M = 0$,

[1] These formulæ agree with those of [89] taking into account that the parameter $\langle \sigma_A v \rangle$ there defined equals 2 times the conventional $\langle \sigma v \rangle_{\rm cosmo}$ here employed.

JHEP06(2014)081

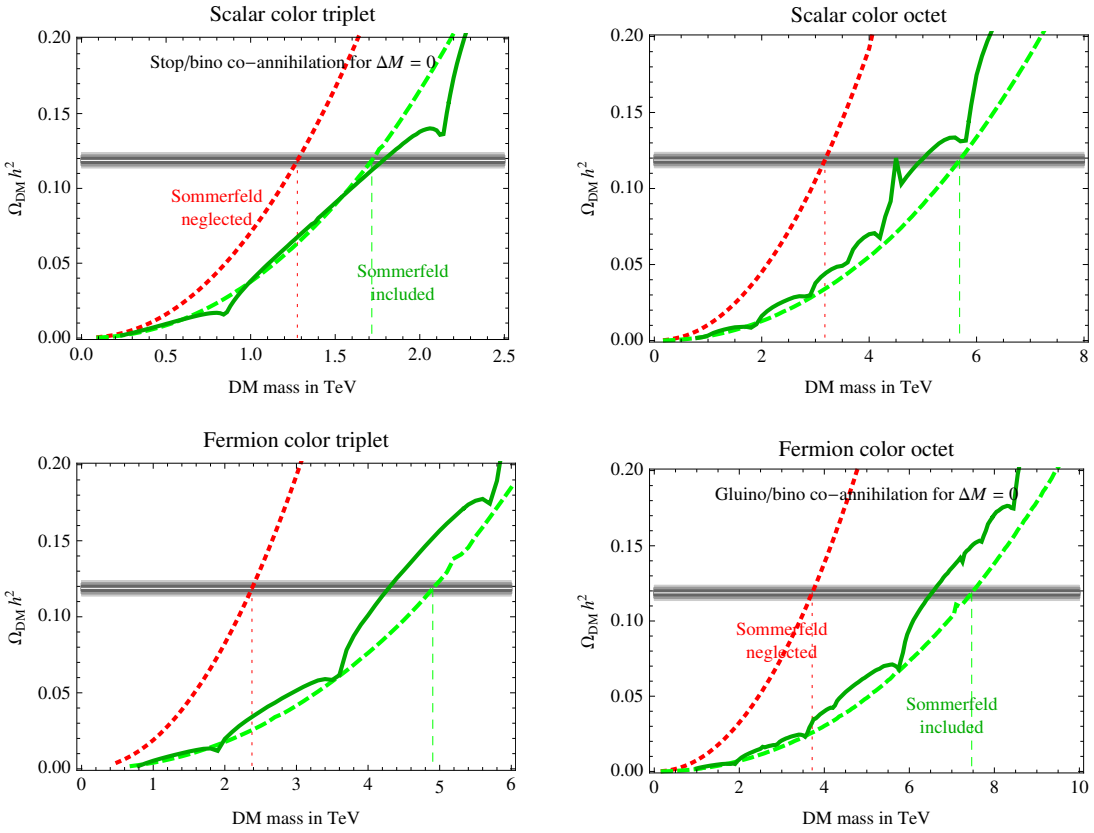

Figure 1. Thermal abundance of DM that co-annihilates with various coloured multiplets (scalar or fermion, triplet or octet) in the limit of mass degeneracy ($\Delta M = 0$). Red dashed line: Sommerfeld corrections neglected. Green dashed line: Sommerfeld corrections included analytically. Green solid line: Sommerfeld corrections and gluon thermal mass included numerically. The horizontal band is the 3σ experimental range for the DM thermal abundance.

then $R = (1 + g_\chi/g_{\chi'})^{-1}$ is about equal to one, as long as the DM number of degrees of freedom is smaller than the one of the coloured χ' dark state. For definiteness, we assume that the DM particle is a Majorana fermion, such as the supersymmetric neutralino, or a complex scalar: $g_\chi = 2$ in both cases. From the analytic expression in eq. (2.13) and the approximate solution in eq. (2.3), one can easily derive a good first estimate of the relic abundance.

We have used a numerical solution to the Boltzmann equations, including also p-wave annihilations, to obtain the DM thermal relic abundance shown by the red curves in figure 1 (DM abundance as a function of $M_{\rm DM}$ for $\Delta M = 0$) and the red bands in the $(M_{\rm DM}, \Delta M)$ plane in figure 2 (values of $M_{\rm DM}$ and of ΔM that correspond to a thermal DM density equal to the observed cosmological density).

However, the tree level annihilation cross sections discussed so far get substantial Sommerfeld corrections due to soft-gluon exchanges between the non-relativistic initial states, as we are now going to describe. After including these corrections, the red curves and bands will shift to the green curves and bands.

JHEP06(2014)081

2.2 QCD Sommerfeld corrections to DM annihilations

The annihilation of two coloured particles, in the non-relativistic limit, is strongly affected by non-perturbative Sommerfeld QCD corrections [90] (see also [91–96]), which describe initial state attraction or repulsion due the strong force. Such corrections have been considered in previous works for gluino annihilation [91] and for stop co-annihilation [97, 98]; however we will find a different result and we will not restrict our attention to the supersymmetric context.

We recall that for a single abelian massless vector with potential $V = \alpha/r$, the Sommerfeld correction $\sigma_{\text{Sommerfeld}} = S\sigma_{\text{perturbative}}$ is given by [90]

$$S(x) = \frac{-\pi x}{1 - e^{\pi x}} \qquad x = \frac{\alpha}{\beta}\,, \tag{2.14}$$

where β is the velocity of the incoming particle. Here $\alpha < 0$ describes an attractive potential that leads to an enhancement $S > 1$, and $\alpha > 0$ describes a repulsive potential that leads to $S < 1$. At higher orders, the QCD potential is roughly given by the tree level potential with the strong coupling renormalised at the RGE scale $\bar{\mu} \approx 1/r$ [99, 100]

$$V(r) = C\frac{\alpha_3(\bar{\mu})}{r}\left[1 + \frac{\alpha_3}{4\pi}\left(\frac{11}{7} + 14(\gamma_E + \ln\bar{\mu}r)\right)\right] \approx C\frac{\alpha_3(\bar{\mu} \approx 1/r)}{r}. \tag{2.15}$$

The constant C is related to the quadratic Casimir of the two particles involved in the interaction. Using a matrix notation, the QCD potential between two particles (scalar or fermions) in the representation R, R' of colour $\mathrm{SU}(3)_c$ with generators T^a_R and $T^a_{R'}$ is

$$V = \frac{\alpha_3}{r}\sum_a T^a_R \otimes T^a_{R'}\,. \tag{2.16}$$

Following ref. [94], the non-abelian Sommerfeld effect can be reduced to a combination of abelian-like Sommerfeld corrections, using group theory decompositions. The non-abelian matrix potential is diagonalised by decomposing the product representation into a sum of irreducible representations Q as $R \otimes R' = \sum_Q Q$:

$$V = \frac{\alpha_3}{2r}\left[\sum_Q C_Q \mathbf{1}_Q - C_R\mathbf{1} - C_{R'}\mathbf{1}\right]\,, \tag{2.17}$$

where C_i is the quadratic Casimir of the representation i. The relevant Casimir for our purposes are $C_1 = 0, C_3 = 4/3, C_8 = 3, C_{10} = C_{\overline{10}} = 6, C_{27} = 8$.

Colour triplet

Annihilations of two colour triplets are decomposed as $3 \otimes \overline{3} = 1 \oplus 8$ and the QCD potential becomes

$$V = \frac{\alpha_3}{r} \times \begin{cases} -\frac{4}{3} & (1) \\ +\frac{1}{6} & (8) \end{cases}\,, \tag{2.18}$$

which is attractive for the singlet two-body state and repulsive for the octet. Next, we need to decompose the total annihilation cross-sections computed in the previous sections into partial cross sections relative to the two-body states.

JHEP06(2014)081

The perturbative triplet + $\overline{\text{triplet}}$ $\to gg$ cross section decomposes into the various sub-channels as: 2/7 in the 1 state, 5/7 in the 8 state (see appendix A). Thereby, the Sommerfeld-corrected cross section is

$$\frac{\sigma(\text{triplet} + \overline{\text{triplet}} \to gg)_{\text{Sommerfeld}}}{\sigma(\text{triplet} + \overline{\text{triplet}} \to gg)_{\text{perturbative}}} = \frac{2}{7} S\left(-\frac{4\alpha_3}{3\beta}\right) + \frac{5}{7} S\left(\frac{\alpha_3}{6\beta}\right). \tag{2.19}$$

Furthermore, if the state χ' is a fermion, it also has s-wave annihilations into two SM quarks, such that

$$\frac{\sigma(\text{F3} + \overline{\text{F3}} \to q\bar{q})_{\text{Sommerfeld}}}{\sigma(\text{F3} + \overline{\text{F3}} \to q\bar{q})_{\text{perturbative}}} = S\left(\frac{\alpha_3}{6\beta}\right). \tag{2.20}$$

Indeed, an ultra-relativistic $q\bar{q}$ pair necessarily has spin $S = 1$, so that all the cross section corresponds to the 8 initial state.

Colour octet

The product of two colour octets decomposes as $8 \otimes 8 = 1_S \oplus 8_A \oplus 8_S \oplus 10_A \oplus \overline{10}_A \oplus 27_S$, where subscripts indicate *A*ntisymmetric and *S*ymmetric combinations. The QCD potential can be written as

$$V = \frac{\alpha_3}{r} \times \begin{cases} -3 & (1_S) \\ -\frac{3}{2} & (8_S, 8_A) \\ 0 & (10_A, \overline{10}_A) \\ +1 & (27_S) \end{cases}, \tag{2.21}$$

which is attractive for the singlet and octet two-particle states. The possible two-body states are classified according to

$$(C, S, L) = (\text{colour, spin, angular momentum}). \tag{2.22}$$

We are interested only in the dominant s-wave annihilations with $L = 0$. For initial scalar octets the anti-symmetric states cannot be in s-wave ($L = 0$), so

$$(8,0) \otimes (8,0) = (1_S, 0) \oplus (8_S, 0) \oplus (27_S, 0) \oplus (\text{states with angular momentum } L \neq 0). \tag{2.23}$$

For initial fermion octets (such as the supersymmetric gluinos) one has

$$\left(8, \frac{1}{2}\right) \otimes \left(8, \frac{1}{2}\right) = (1_S, 0) \oplus (8_S, 0) \oplus (8_A, 1) \oplus (10_A, 1) \oplus (\overline{10}_A, 1) \oplus (27_S, 0). \tag{2.24}$$

With the group-theoretical algebra outlined in appendix A, we find that the perturbative octet + octet $\to gg$ cross section decomposes into the various sub-channels as: 1/6 in the 1_S state, 1/3 in the 8_S state and 1/2 in the 27_S state, while the antisymmetric 8_A, 10_A and $\overline{10}_A$ states do not contribute. Since C is conserved by QCD interactions, an s-wave ($L = 0$) initial state of two fermions ($C = (-1)^{L+S}$) can annihilate into $N_V = 2$ vectors ($C = (-1)^{N_V} = +1$) only if $S = 0$. Therefore, a scalar and fermion colour octet have the same Sommerfeld-corrected cross section into gluons:

$$\frac{\sigma(\text{octet} + \text{octet} \to gg)_{\text{Sommerfeld}}}{\sigma(\text{octet} + \text{octet} \to gg)_{\text{perturbative}}} = \frac{1}{6} S\left(-\frac{3\alpha_3}{\beta}\right) + \frac{1}{3} S\left(-\frac{3\alpha_3}{2\beta}\right) + \frac{1}{2} S\left(\frac{\alpha_3}{\beta}\right). \tag{2.25}$$

JHEP06(2014)081

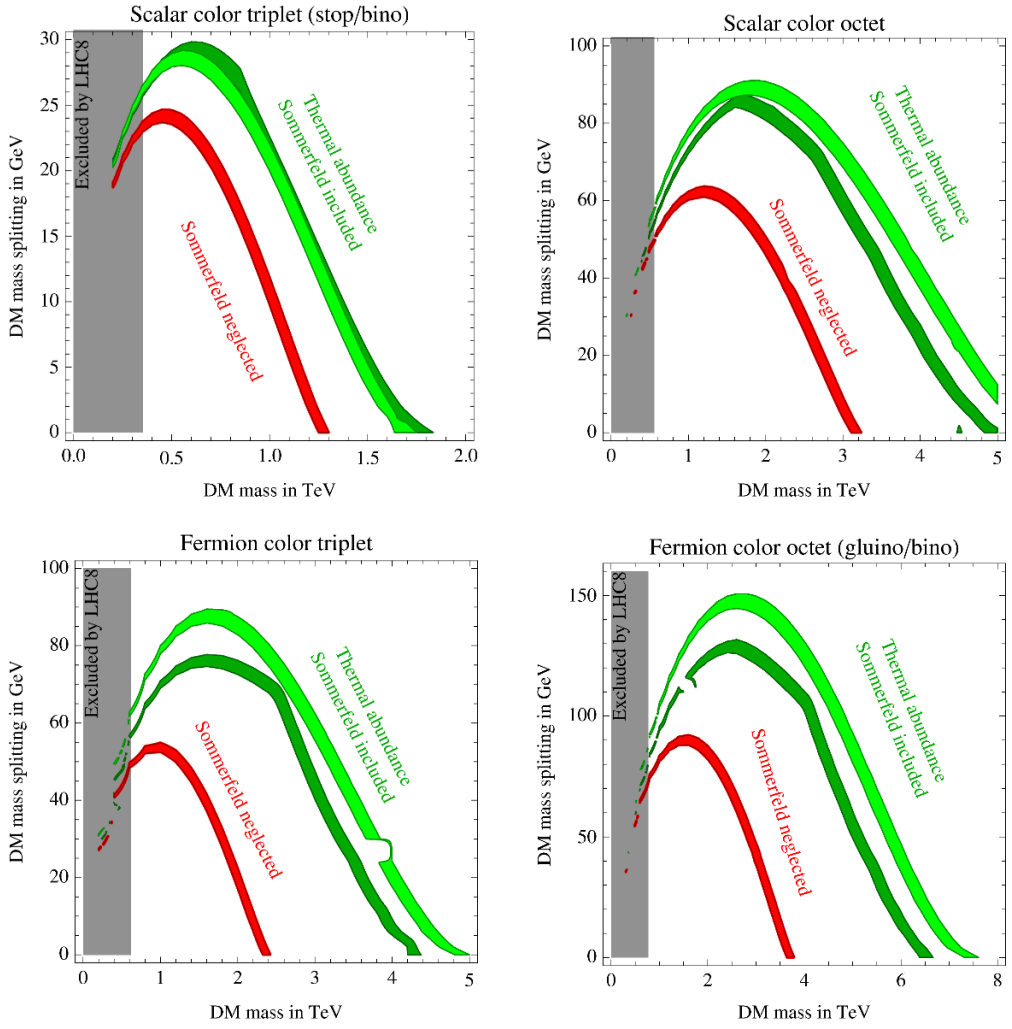

Figure 2. The coloured bands show the region in the $M_{\rm DM}$–ΔM plane where the correct relic abundance is achieved for DM co-annihilating with a scalar/fermion colour-triplet/octet partner. Red: Sommerfeld corrections neglected. Light green: Sommerfeld corrections included analytically. Dark green: Sommerfeld corrections and gluon thermal mass included numerically. The LHC 90%CL exclusion is also shown as a vertical grey band. The DM is assumed to be a Majorana fermion. The case of scalar DM is very similar.

Furthermore, fermion octets also have s-wave annihilations into SM quarks, which for ultra-relativistic quarks form a $(8_A, 1)$ initial state, so that one simply has

$$\frac{\sigma(\mathrm{F8}+\mathrm{F8}\to q\bar{q})_{\rm Sommerfeld}}{\sigma(\mathrm{F8}+\mathrm{F8}\to q\bar{q})_{\rm perturbative}} = S\left(-\frac{3\alpha_3}{2\beta}\right). \tag{2.26}$$

2.3 Results for DM co-annihilations with a coloured partner

By approximating the QCD potential as proportional to $1/r$ (i.e. by renormalising α_3 at some fixed relevant scale in eq. (2.15)), the above equations provide a simple analytical approximation for the Sommerfeld corrections S. In figure 2 we show in light green the

JHEP06(2014)081

bands in the $(M_{\rm DM}, \Delta M)$ plane where the DM thermal abundance reproduces the observed value within ± 3 standard deviations.

We also compute the Sommerfeld correction in a more accurate way, by accounting for two more effects:

- The full QCD potential taking into account the scale dependence of the QCD coupling constant, as in eq. (2.15);
- Finite-temperature effects, which provide a zero-momentum thermal mass $m_3 = \sqrt{2} g_3 T$ to the gluon, transforming the QCD potential into a Yukawa potential.

The Coulomb approximation of eq. (2.14) no longer holds, and the Sommerfeld factor S needs to be computed numerically by finding the relevant wave-functions with the full potential, after solving the associated Schrödinger equation.

Our full computation leads to the solid green line in figure 1 (relic abundance as a function of $M_{\rm DM}$ for $\Delta M = 0$) and to the bands in dark green in figure 2 (relation between $M_{\rm DM}$ and ΔM that corresponds to DM density). The irregular peak structure, especially visible in figure 1, corresponds to the appearance of two-body bound states with zero binding energy. Note also that from the results in figure 1 one can easily extract the Sommerfeld-corrected thermal relic abundance of a stable LSP gluino. This is obtained by multiplying the lines shown in the bottom-right panel (fermion colour octet) of figure 1 by the factor $R = 8/9$.

For vanishing mass splitting in the dark sector, $\Delta M = 0$, the Sommerfeld corrections significantly increase the particle mass needed to reproduce the observed DM abundance:

	Scalar triplet	Fermion triplet	Scalar octet	Fermion octet
$M_{\rm DM}$ (Sommerfeld neglected)	1.3 TeV	2.4 TeV	3.2 TeV	3.7 TeV
$M_{\rm DM}$ (Sommerfeld included)	1.7 TeV	$4-5$ TeV	$5-6$ TeV	$7-8$ TeV
LHC lower bound at 90% CL	0.35 TeV	0.62 TeV	0.56 TeV	0.77 TeV

(2.27)

The lower row shows the present bounds from searches at the LHC, computed as follows. Once produced at the LHC, the coloured χ' decays into DM (escaping the detector as missing energy) with the emission of a jet. We focus on the case where ΔM is so low that the radiated jet is too soft to be triggered. For larger ΔM, it would be possible to use other search channels with multiple jets and missing energy. The constraints on χ' production are extracted from the mono-jet DM searches relying on QCD radiation to trigger the event [101].

We simulated with MadGraph [102] the tree-level process $pp \to \chi'\chi'$+jet (at $\sqrt{s} = 8$ TeV), requiring the leading jet to have $p_T > 110$ GeV, $|\eta| < 2.4$, to reproduce the analysis in [103, 104], corresponding to data with integrated luminosity of $\mathcal{L} = 19.5\,{\rm fb}^{-1}$. Then we used the number of observed and background events reported for the region with $E_{\rm T}^{\rm miss} > 400$ GeV, and placed the observed 90% CL exclusion limit on $M_{\chi'} = M_{\rm DM} + \Delta M$ by requiring

$$\chi^2 = \frac{\left[N_{\rm obs} - N_{\rm bkg} - N_{\chi'}(M_{\rm DM} + \Delta M)\right]^2}{N_{\chi'}(M_{\rm DM} + \Delta M) + N_{\rm bkg} + \sigma^2_{\rm bkg}} = 2.71\,, \tag{2.28}$$

JHEP06(2014)081

where $\sigma_{\rm bkg}$ is the uncertainty on the background estimation. We computed the number of signal events $N_{\chi'}$ simply as the integrated luminosity $\mathcal{L}$ times the signal cross section (with unit efficiency and acceptance).

Future searches at the LHC will be able to extend the reach for testing DM that co-annihilates with a coloured partner. However, figure 2 shows that the LHC will not be able to probe the entire parameter space allowed by thermal freeze-out. The full exploration of DM co-annihilating with a coloured partner requires higher energies. It is interesting that a future pp collider with $\sqrt{s} \sim 100\,\text{TeV}$ will play an important role in the exploration of the mass range favoured by DM thermal abundance [105].

3 DM annihilating through a SM mediator

In this section we consider situations in which the mediator of interactions between DM and quarks is a SM particle, rather than a speculative particle from the dark sector. Given that DM is neutral and has no colour, the candidates for the role of mediator are the Z (considered in section 3.1) and the Higgs boson (considered in section 3.2).

3.1 DM coupled to the Z

We start by assuming that the DM particle is coupled to the Z boson. At low energies, the Lagrangian interaction of the Z boson to a current of fermions f and scalars s is

$$\mathcal{L} = -Z_\mu J^\mu_Z\,, \qquad J^Z_\mu = \frac{g_2}{\cos\theta_{\rm W}}\left[\sum_f [\bar f \gamma_\mu (g_V^f + \gamma_5 g_A^f) f] + \sum_s g_s [s^*(i\partial_\mu s) - (i\partial_\mu s^*)s]\right], \quad (3.1)$$

where g_2 and $\theta_{\rm W}$ are the $\mathrm{SU}(2)_L$ gauge coupling and weak angle. For the SM fermions one has the well-known result $g_V = \frac{1}{4} - \frac{2}{3}\sin^2\theta_{\rm W}$ and $g_A = -\frac{1}{4}$ for up-type quarks and $g_V = -\frac{1}{4} + \frac{1}{3}\sin^2\theta_{\rm W}$ and $g_A = \frac{1}{4}$ for down-type quarks. Since the coupling of each chiral fermion to the Z is proportional to $T_3 - Q\sin^2\theta_{\rm W} = Q\cos^2\theta_{\rm W} - Y$, the coupling of the DM particle, which is neutral ($Q = 0$), is proportional to its hypercharge. In our effective Lagrangian, we consider $g_V^{\rm DM}$, $g_A^{\rm DM}$ or $g_s^{\rm DM}$ as free parameters that describe the DM couplings. Small values of the DM couplings to Z can be obtained if the DM is a mixture between a state with $Y = 0$ and a state with $Y \neq 0$, or if DM does not couple directly to Z, but only to a Z' boson that mixes with the Z.

At energies larger than M_Z, we need to complete in a gauge-invariant way the couplings in eq. (3.1). This is obtained by observing that, on the Higgs vacuum,

$$-\frac{4i\cos\theta_{\rm W}}{g_2\ v^2}\ H^\dagger D_\mu H\Big|_{H=\langle H\rangle} = Z_\mu\,, \quad (3.2)$$

where H is the full Higgs doublet and $v = 246\,\text{GeV}$. Thus, the simplest gauge invariant completion of the coupling between the Z boson and fermonic or scalar DM is

$$\mathcal{L} = \frac{4i}{v^2}(H^\dagger D^\mu H)\left[\bar\psi_{\rm DM}\gamma_\mu(g_V^{\rm DM} + \gamma_5 g_A^{\rm DM})\psi_{\rm DM} + g_s^{\rm DM}\big(s^*_{\rm DM}(i\partial_\mu s_{\rm DM}) - (i\partial_\mu s^*_{\rm DM})s_{\rm DM}\big)\right]. \quad (3.3)$$

Indeed, these are the lowest-dimension operators leading to the interactions in eq. (3.1).

JHEP06(2014)081

Direct detection

Concerning direct detection, by integrating out the Z at tree level one obtains the effective Lagrangian $\mathcal{L}_{\rm eff} = -J_Z^2/2M_Z^2$. By taking the nucleon matrix element and the non-relativistic limit we obtain the Lagrangian

$$\mathcal{L}_{\text{non rel}} = \sum_{N}^{n,p} \sum_{i=1}^{12} c_i^N \mathcal{O}_i^N \,, \tag{3.4}$$

where the first sum runs over $N = \{n, p\}$ and the second sum over the 12 most general DM/nucleon non-relativistic operators [9, 31]. Only a few of them are generated in our case.

- Scalar DM and fermion DM with vector interactions produces the dominant spin-independent operator $\mathcal{O}_1^N = 1$ with coefficients

$$c_1^n = 0.27 g^{\rm DM} \frac{M_{\rm DM} m_N}{M_Z^2}, \qquad c_1^p = -0.03 g^{\rm DM} \frac{M_{\rm DM} m_N}{M_Z^2} \,, \tag{3.5}$$

  where g is either $g_V^{\rm DM}$ or $g_s^{\rm DM}$. All other operators give negligible corrections.

- Fermion DM with axial interactions produces, as main effect, the dominant spin-dependent operator $\mathcal{O}_4^N = \vec{S}_{\rm DM} \times \vec{s}_N$:

$$c_4^n = c_4^p = 0.38 g_A^{\rm DM} \frac{M_{\rm DM} m_N}{M_Z^2}. \tag{3.6}$$

  It also produces $\mathcal{O}_8^N = \vec{S}_{\rm DM} \cdot \vec{v}_\perp$, which is spin-independent but suppressed by the DM transverse velocity $\vec{v}_\perp$. In view of the coefficients

$$c_8^n = 0.54 g_A^{\rm DM} \frac{M_{\rm DM} m_N}{M_Z^2}, \qquad c_8^p = 0.06 g_A^{\rm DM} \frac{M_{\rm DM} m_N}{M_Z^2} \tag{3.7}$$

  such operator is somehow less relevant than $\mathcal{O}_4^N$, but not irrelevant.[2]

We derive the bound from all direct detection experiments by employing the public code of ref. [106]. The bounds are dominated by the LUX experiment [107]. The effect of loop corrections that transform spin-dependent interactions into spin-independent cross section is irrelevant, since it can affect our bound on $g_A^{\rm DM}$ only if DM is lighter than a few GeV [108].

Thermal abundance

We compute the relic abundance using the interaction between DM and SM particles given in eq. (3.3). This interaction contributes to DM annihilation via s-channel Z exchange and also to direct annihilation into a pair of Higgs and/or gauge bosons. We perform

[2] Fermion DM with axial interactions also produces other operators, $\mathcal{O}_7^N = \vec{s}_N \cdot \vec{v}_\perp$ and $\mathcal{O}_9^N = i\vec{S}_{\rm DM} \cdot (\vec{s}_N \times \vec{q})$, which have a negligible effect because spin-dependent and suppressed.

JHEP06(2014)081

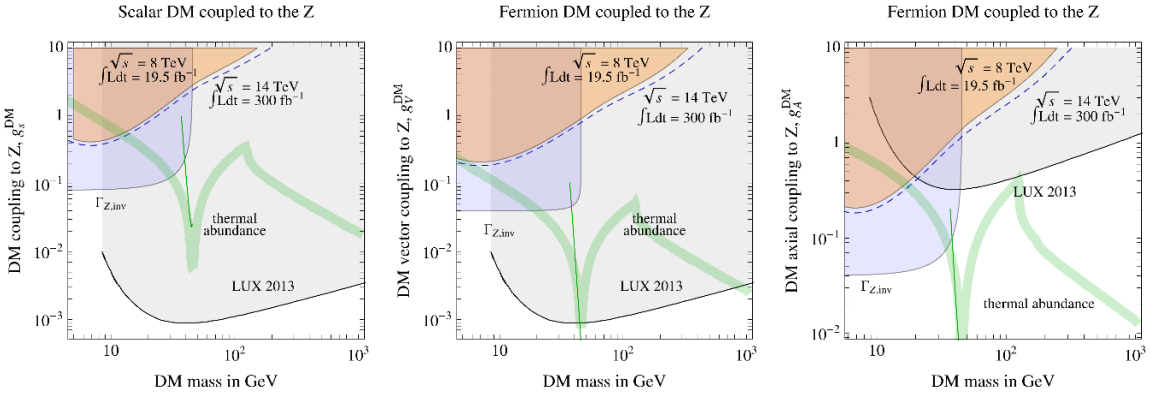

Figure 3. *DM coupled to the Z.* Regions of DM mass $M_{\rm DM}$ and Z couplings ($g_s^{\rm DM}$, $g_V^{\rm DM}$, $g_A^{\rm DM}$): the orange region is excluded at 90% CL by ATLAS mono-jet searches at LHC8, with forecast for LHC14 (dashed blue line); the grey region is excluded at 90% CL by LUX 2013 direct searches; the blue region is excluded by the Z-invisible width constraint $\Gamma_{Z,\rm inv} < 2$ MeV. The green solid curve corresponds to a thermal relic abundance via Z-coupling annihilation equal to the observed DM density (the thick curve is the off-shell estimation; the thin curve is the on-shell computation).

a full calculation of the relic abundance, including all annihilation channels. The approximation of retaining only the dimension-6 interaction in eq. (3.3) is valid as long as the effective energy scale $(v/\sqrt{g_{V,A,s}^{\rm DM}})$ is much larger than the DM mass. This implies $g_{V,A,s}^{\rm DM} \ll 0.24\ (500\,{\rm GeV}/M_{\rm DM})^2$, which is valid in the region of interest. However, if new physics is not far from $M_{\rm DM}$, new interactions and new annihilation channels open up, presumably reducing the thermal relic abundance. These effects are completely model-dependent.

The computation of the thermal relic DM abundance becomes model-independent in the kinematic region $M_{\rm DM} \approx M_Z/2$, since the annihilation cross section is dominated by the Z-resonance. We postpone the discussion of this interesting case to section 4, where we will show that the DM abundance can be simply computed in terms of the Z decay width rather than in terms of DM annihilations.

Results

In figure 3 we compare the LHC sensitivity with the current bounds. In the plane (DM mass, DM coupling to Z) we show:

1. The bounds from direct detection, dominated by the LUX experiments (regions shaded in grey). The bounds on $g_V^{\rm DM}$ and $g_s^{\rm DM}$ are quite strong (around 10^{-3} for DM mass around 100 GeV), while $g_A^{\rm DM}$, which leads to spin-dependent interactions, is less constrained (typically $g_A^{\rm DM} \lesssim 0.3$ for $M_{\rm DM} \approx 100\,{\rm GeV}$). We see that direct detection experiments severely constrain the vector coupling $g_V^{\rm DM}$ and the scalar coupling $g_s^{\rm DM}$, and are presently probing the region $g_A^{\rm DM} \sim 1$.

2. The LEP bounds from the invisible Z width, $\Gamma_{Z,\rm inv} < 2\,{\rm MeV}$. This bound, shown in light blue, implies $g_{V,A}^{\rm DM} \lesssim 0.04$, $g_s^{\rm DM} \lesssim 0.08$ if $M_{\rm DM} < M_Z/2$.

JHEP06(2014)081

3. The present bound from LHC mono-jet searches, extracted with the procedure described in section 2.3. We see that such bounds can never be competitive with the combined limits from LUX and LEP.

4. Our estimate on the future sensitivity of LHC at $\sqrt{s} = 14\,\text{TeV}$ with an integrated luminosity of $300\,\text{fb}^{-1}$. By simulating the sample and rescaling the corresponding statistical error with the square-root of the number of events we find that only a modest improvement is possible. New strategies for reducing the systematic error and improving background rejection are necessary for the LHC to give competitive results.

5. The curve that corresponds to a thermal DM density equal to the cosmological density (green curve). We observe that a thermal abundance from pure Z coupling is ruled out for scalar DM, while some regions are still allowed for fermion DM, most notably for axial couplings and in the window around the near-resonant region (that will be discussed in section 4). However, we stress that the relic abundance, computed here using the effective interaction in eq. (3.3), is very sensitive to new-physics effects, especially in the high-mass region. In particular, the decrease of the green line with the DM mass is only a consequence of the non-renormalisable contact interactions. New particles and new interactions can completely modify the behaviour of the thermal-abundance constraint. Hence, the green curve in figure 3 is only meant to be indicative of the effective-theory regime.

3.2 DM coupled to the Higgs

The case of DM that couples to the SM sector only though interactions with the Higgs boson has been discussed extensively in the literature [65–86]. Here we assume that DM is either a real scalar ($s_{\rm DM}$) or a Majorana fermion ($\psi_{\rm DM}$) coupled to the physical Higgs field h at low energies as

$$\mathcal{L} = -hJ_h\,, \qquad J_h = \frac{1}{\sqrt{2}}\left[\sum_f y_f \bar{f} f + \bar{\psi}_{\rm DM}(y_{\rm DM} + i y^P_{\rm DM}\gamma_5)\psi_{\rm DM} + \frac{\lambda_{\rm DM} v}{2} s^2_{\rm DM}\right]. \tag{3.8}$$

The SM fermions f have the usual Yukawa couplings y_f and we parameterise the DM couplings to the Higgs as $\lambda_{\rm DM}$, $y_{\rm DM}$, $y^P_{\rm DM}$.

We can complete the effective interaction in eq. (3.8) in a straightforward way, since $H^\dagger H/v = \sqrt{2}h + \ldots$. Hence, the simplest recipe to express the DM coupling to Higgs boson in terms of gauge-invariant quantities is

$$\mathcal{L} = -H^\dagger H\left[\bar{\psi}_{\rm DM}\frac{(y_{\rm DM} + i y^P_{\rm DM}\gamma_5)}{2v}\psi_{\rm DM} + \frac{\lambda_{\rm DM}}{4} s^2_{\rm DM}\right]. \tag{3.9}$$

Note that the coupling of scalar DM to the Higgs doublet can be expressed in terms of a renormalisable interaction, while the coupling of fermonic DM involves a dimension-5 operator.

JHEP06(2014)081

Direct detection

By integrating out the Higgs boson, one obtains the effective Lagrangian $\mathcal{L}_{\rm eff} = J_h^2/2M_h^2$ that describes direct detection. Employing again the non-relativistic nucleon Lagrangian of eq. (3.4) we find:

- The $\lambda_{\rm DM}$ coupling of scalar DM generates the dominant spin-independent effective non-relativistic operator $\mathcal{O}_1^N = 1$ with coefficients

$$c_1^n \approx c_1^p = -0.45\lambda_{\rm DM}\frac{m_N v}{M_h^2}. \tag{3.10}$$

- The $y_{\rm DM}$ coupling of fermion DM also generates $\mathcal{O}_1^N$ with

$$c_1^n \approx c_1^p = -1.8 y_{\rm DM}\frac{m_N M_{\rm DM}}{M_h^2}\,. \tag{3.11}$$

- The pseudo-scalar coupling $y^P_{\rm DM}$ only produces the operator $\mathcal{O}_{11}^N = i\vec{S}_{\rm DM}\cdot\vec{q}$, which is spin-dependent and suppressed by the transferred momentum $\vec{q}$:

$$c_{10}^n \approx c_{10}^p \approx 0.26\frac{y^P_{\rm DM} m_N}{M_h^2}. \tag{3.12}$$

  As a consequence, there are no limits on perturbative values of $y^P_{\rm DM}$.

Thermal abundance

The relic abundance is computed using the interaction in eq. (3.9), which contributes to DM annihilation through s-channel Higgs exchange and through processes with two Higgs or longitudinal gauge bosons in the final state. We include these annihilation channels in our computation. In the case of fermionic DM, the approximation of keeping only the dimension-5 operator in eq. (3.9) is justified as long as $y_{\rm DM} \ll 0.5\ (500\,{\rm GeV}/M_{\rm DM})$.

Results

In figure 4 we compare the LHC sensitivity with current bounds, in the plane (DM mass, DM coupling to h), finding the following results.

1. The bounds from direct detection are dominated by the LUX experiments (regions shaded in grey). We see that direct detection experiments are severely constraining the scalar couplings $\lambda_{\rm DM}, y_{\rm DM}$, while the pseudo-scalar interaction is completely out of reach at the moment.

2. If $M_{\rm DM} < M_h/2$, the main constraint is due to the Higgs invisible width, $\Gamma_{h,\rm inv}/\Gamma_h \lesssim 20\%$, which gives $\lambda_{\rm DM}, y_{\rm DM}, y^P_{\rm DM} \lesssim 10^{-2}$, taking $\Gamma_h = 4.2\,{\rm MeV}$ for $M_h = 125.6\,{\rm GeV}$.

3. In the opposite regime, $M_{\rm DM} > M_h/2$, one can consider different Higgs production mechanisms at the LHC: gluon fusion accompanied by mono-jet, VBF, Higgs-strahlung from W/Z. We considered the first case (gluon fusion) and assumed $M_h = 125.6\,{\rm GeV}$. However, the parameter space region accessible by LHC mono-jet searches is either already excluded by direct detection $(\lambda_{\rm DM}, y_{\rm DM})$ or involves unreasonably large couplings $(y^P_{\rm DM})$.

JHEP06(2014)081

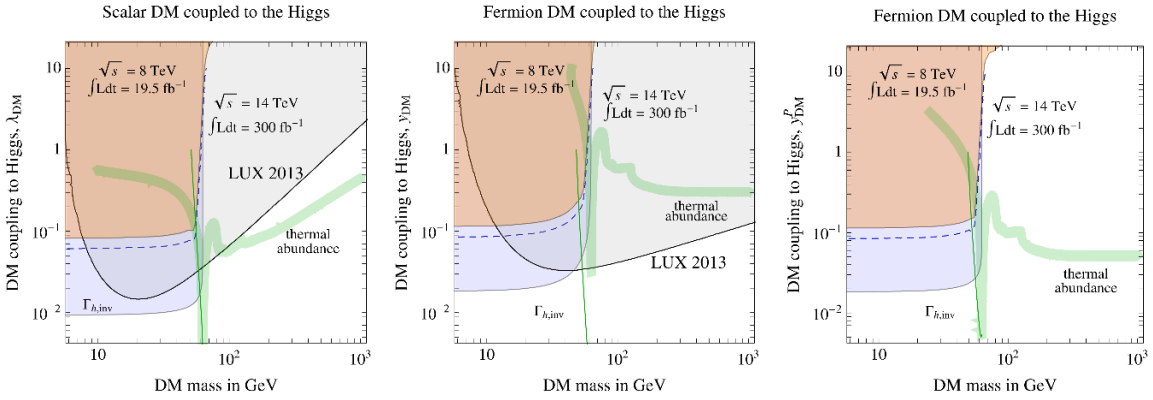

Figure 4. *DM coupled to the Higgs.* Regions of DM mass $M_{\rm DM}$ and Higgs couplings ($\lambda_{\rm DM}$, $y_{\rm DM}$, $y^P_{\rm DM}$): the orange region is excluded at 90% CL by ATLAS mono-jet searches at LHC8, with forecast for LHC14 (dashed blue line); the grey region is excluded at 90% CL by LUX 2013 direct searches; the blue region is excluded by the Higgs invisible width constraint $\Gamma_{h,\rm inv}/\Gamma_h < 20\%$. The green solid curve corresponds to a thermal relic abundance via Higgs-coupling annihilation equal to the observed DM density (the thick curve is the off-shell estimation; the thin curve is the on-shell computation).

4. As for the case of DM coupling to the Z, the present bound from LHC mono-jet searches, extracted with the procedure described in section 2.3, are not competitive with the combined limits from LUX and Higgs invisible width, not even projecting the sensitivity of LHC14 with 300 fb^{-1}.

5. The case of a DM coupling to the Higgs responsible for the correct relic abundance is ruled out for fermionic DM (but allowed for pseudoscalar coupling when $M_{\rm DM} > M_h/2$). For scalar DM, this possibility is still viable for $M_{\rm DM} \gtrsim 100\,{\rm GeV}$. A small mass window around the resonant Higgs exchange is allowed, and this case will be discussed in section 4. However, we recall again that the thermal abundance lines in figure 4 bear a dependence on the completion of the theory and our calculation is based on an effective-theory regime with couplings defined by eq. (3.9). In particular, for fermonic DM, the green line in figure 4 is approximately independent of the DM mass in the high-mass region; this result is characteristic of dimension-5 interactions. New particles and new interactions can easily reduce the cosmological abundance of the DM particle coupled to the Higgs.

4 DM freeze-out via decays

A special case occurs when the DM annihilation cross section relevant for the thermal relic abundance is resonantly enhanced by the mediator exchange in the s-channel. This applies when the DM mass is about $M_Z/2 = 45.6\,{\rm GeV}$ or $M_h/2 = 63\,{\rm GeV}$, but our considerations apply to the case of a generic mediator M (such as extra Higgses present in supersymmetric models or Z' gauge bosons). We will consider a mediator M with g_M degrees of freedom, with mass M_M slightly larger than $2M_{\rm DM}$, with branching ratio ${\rm BR}_{\rm DM}$ into a pair of DM

JHEP06(2014)081

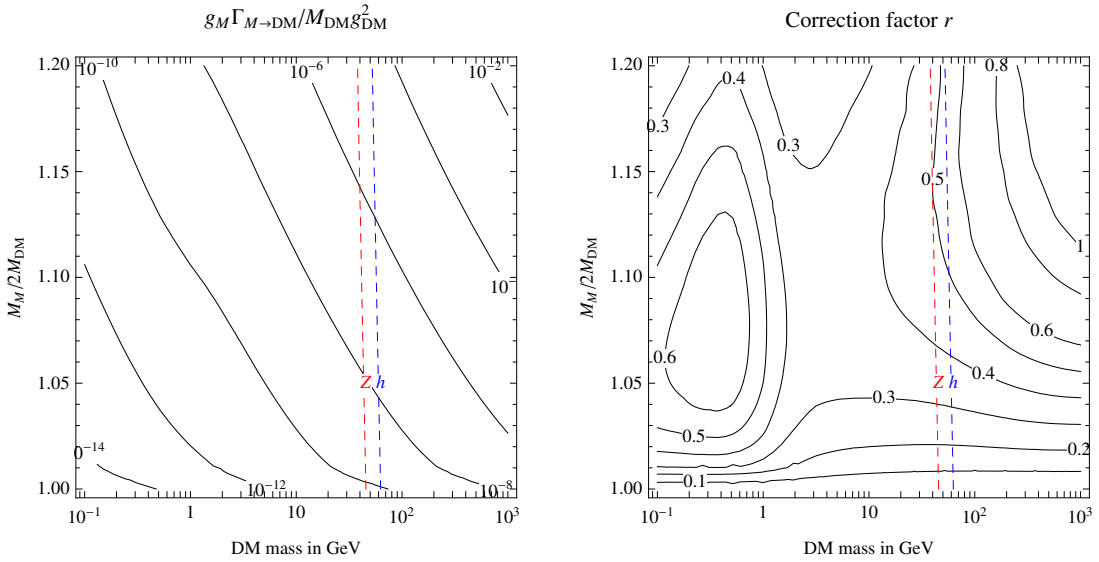

Figure 5. *DM freeze-out via decays* of a generic mediator particle M. The dashed curves emphasise the special cases where the mediator is the Z (red) or the Higgs boson (blue). Left panel: value of $(g_M/g^2_{\mathrm{DM}})\Gamma_{M\to\mathrm{DM}}/M_{\mathrm{DM}}$ such that decays into DM particles reproduce the observed DM abundance. Right panel: the order-one factor r that gives the precise normalisation of the DM thermal abundance via decays, as defined in eq. (4.4).

particles and $1-\mathrm{BR}_{\mathrm{DM}}$ into light SM particles. The DM particle has g_{DM} degrees of freedom. If the DM mass differs from half of the mediator mass by less than its width, then the cross section becomes fairly model-independent and is approximated by the Breit-Wigner formula. The thermal average γ_A of a resonant annihilation cross section can be simplified as follows.

The total thermally averaged DM annihilation rate γ_A can be decomposed as the contribution of the on-shell resonant term plus the remaining off-shell contribution γ_A^{sub}:

$$\gamma_A = \gamma_A^{\mathrm{on-shell}} + \gamma_A^{\mathrm{off-shell}}. \tag{4.1}$$

Formally, $\gamma_A^{\mathrm{on-shell}}$ can be computed by approximating the Breit-Wigner as a Dirac δ function. As expected, the scattering rate reduces to a much simpler object: the thermal average γ_D of the decay rate of the mediator,

$$\gamma_A^{\mathrm{on-shell}} = \mathrm{BR}_{\mathrm{DM}}(1-\mathrm{BR}_{\mathrm{DM}})\gamma_D. \tag{4.2}$$

The term $\gamma_A^{\mathrm{off-shell}}$ can be computed using a subtracted propagator for the mediator particle M, as described in [109]. However, in the context of section 3, the off-shell contribution is model-dependent.

We focus on the model-independent on-shell term, which is described by the decay rate. In this approximation one has the simple result

$$\gamma_A \approx \mathrm{BR}_{\mathrm{DM}}\gamma_D = n_M^{\mathrm{eq}}\frac{K_1(M_M/T)}{K_2(M_M/T)}\Gamma_{M\to\mathrm{DM}} \overset{T\ll M_{\mathrm{DM}}}{\simeq} g_M\Gamma_{M\to\mathrm{DM}}\left(\frac{M_M T}{2\pi}\right)^{3/2} e^{-M_M/T}. \tag{4.3}$$

JHEP06(2014)081

We considered the relevant non-relativistic limit, and we notice that γ_D has a different dependence on T than the standard annihilation rate (proportional to $e^{-2M_{\rm DM}/T}$), so the usual approximation in terms of the non-relativistic parameter σv is not appropriate. Rather, the DM abundance is determined in terms of the width $\Gamma_{M\to DM}$, such that the final DM number abundance is roughly given by $n_{\rm DM}/s \sim H/\Gamma_{M\to \rm DM}$ where H is the Hubble constant at $T \sim M_{\rm DM}$. By solving the Boltzmann equation for the DM abundance keeping only the on-shell term we find the precise result

$$\frac{\Omega_{\rm DM}h^2}{0.1187} = r\frac{g_{\rm DM}^2 10^{-12}\,\text{GeV}}{g_M \Gamma_{M\to \rm DM}}\left(\frac{M_{\rm DM}}{\text{GeV}}\right)^3 e^{-2z_f \Delta M/M_{\rm DM}}\,. \tag{4.4}$$

We have defined $\Delta M = M_M - 2M_{\rm DM}$ and fixed $z_f \equiv 25$. Then r is an order-one factor plotted in figure 5 (right panel), obtained from the numerical solution of the Boltzmann equations. As in the annihilation case, the relevant rate is averaged over the DM components and summed over the SM components. In the left panel of figure 5, we show the invisible width of the mediator, in units of its mass, that corresponds to the correct DM abundance via decays.

We can now apply our results to the case in which the mediator M is either the Z or the Higgs boson. For the various couplings considered in section 3, the decay widths into DM particles are

$$\Gamma_{Z\to \rm DM} = \frac{g_2^2 M_Z}{12\pi\cos^2\theta_{\rm W}}\sqrt{1-\frac{4M_{\rm DM}^2}{M_Z^2}}\begin{cases} g_V^{\rm DM2}(1+2M_{\rm DM}^2/M_Z^2) \\ g_A^{\rm DM2}(1-4M_{\rm DM}^2/M_Z^2) \\ g_s^2(1/4 - M_{\rm DM}^2/M_Z^2) \end{cases}, \tag{4.5}$$

$$\Gamma_{h\to \rm DM} = \frac{M_h}{16\pi}\sqrt{1-\frac{4M_{\rm DM}^2}{M_h^2}}\begin{cases} y_{\rm DM}^2(1-4M_{\rm DM}^2/M_h^2) \\ y_{\rm DM}^{P2} \\ \frac{1}{2}\lambda_{\rm DM}^2(v/M_h)^2 \end{cases}. \tag{4.6}$$

The values of the invisible branching ratios needed to reproduce the DM abundance are shown in figure 6. This result holds as long as the on-shell contribution that we are considering dominates over the neglected off-shell contribution, which occurs typically for $\Delta M \lesssim 0.2 M_{\rm DM}$. As shown in figure 6, a broad range of experimentally unexplored Z or Higgs invisible widths could account for DM via thermal freeze-out of decays. This result gives good motivations for improved measurements of the invisible width of the Z boson (e.g. in GigaZ) and of the Higgs boson (in upcoming LHC data and in future Higgs factories).

5 Summary

The search for DM is one of the most exciting goals of the LHC. However, the path that DM hunters should follow is not obvious because of our ignorance about the nature of the DM and the lack of experimental evidence for new particles beyond the SM. In this situation, experiments at the LHC must pursue a diversified strategy of searches. In this paper we have considered some benchmark cases that offer prospects for DM discovery and that can guide experimental searches without full commitment to specific models.

JHEP06(2014)081

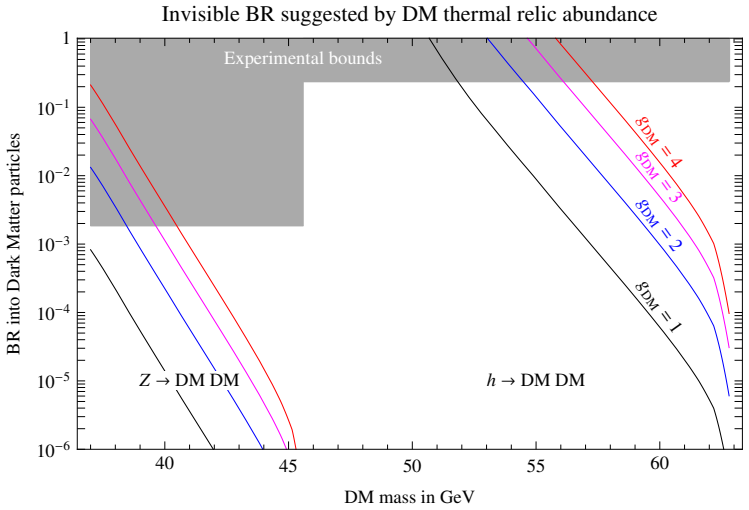

Figure 6. Values of the invisible Z and h branching ratio into DM particles needed to reproduce the DM abundance via thermal freeze-out of decays. We consider DM with $g_{\rm DM} = 1$ (black curve), 2 (blue), 3 (magenta), 4 (red) degrees of freedom.

DM co-annihilating with a coloured partner. As a first benchmark case, we have considered a situation in which the DM thermal relic abundance is determined by co-annihilation with a coloured particle. This possibility is very favourable for the LHC, because of the large QCD cross section for producing the DM partner. However, the near mass degeneracy with the DM particle makes this search at the LHC experimentally challenging, requiring either extra jets to tag the event and/or the identification of soft decay products. Co-annihilation with coloured partners can occur in many models with new particles at the weak scale, including supersymmetry. Interesting examples are the cases of near-degenerate neutralino-stop, neutralino-sbottom, or neutralino-gluino. However, even without making any model-dependent assumption, the case of DM co-annihilating with a coloured partner can be fully characterised by: the quantum numbers of the DM partner (spin and colour representation), its mass, and its mass difference with the DM particle. In terms of these parameters, one can determine the DM relic abundance and the signals at the LHC. An important result of our study is the calculation of the Sommerfeld corrections to the annihilation rates, taking into account the colour decomposition of the various initial states. As a byproduct, we obtain the correct expression of the Sommerfeld factor for gluino LSP annihilation. Our results for the DM relic abundance are summarised in figures 1 and 2. We find that future LHC searches will be able to probe a large region of parameters that is still unexplored and that leads to a correct DM density. However, LHC cannot give a conclusive answer to the viability of DM co-annihilating with coloured partners. Indeed, a correct thermal relic density can be achieved even for DM masses as large as 5 TeV (for a fermion colour triplet partner) or 10 TeV (for a fermion colour octet partner). Future hadron colliders operating at 100 TeV energies are necessary to complete the exploration of these models.

DM annihilating through a SM mediator. In a large class of models the DM particle is coupled to the SM sector only through the Z or Higgs boson. In this case, the mass

JHEP06(2014)081

of the mediator is known, but we treat the couplings between the DM particle and the Z or Higgs boson as free parameters. Although the thermal DM abundance is somehow model-dependent, we can compare the reach of the different experimental strategies. We find that, taking into account the LEP bound on the Z invisible width and the LUX 2013 data, searches at the LHC for DM coupled to the Z are not sufficiently competitive. The situation is more promising for DM coupled to the Higgs because, for $M_{\rm DM} < M_h/2$, searches for invisible Higgs decays are competitive with direct searches in underground experiments. Our findings are illustrated in figures 3 and 4. In spite of the negative results for DM coupled to the Z, improvements at the LHC in all missing-energy channels are motivated, independently of the relic density prediction and the LUX 2013 results. Indeed, DM could have a non-thermal origin (evading the relic abundance constraint) or could have a clumped distribution in the galactic halo (weakening the constraints from direct DM searches).

DM freeze-out via decays. An especially interesting situation occurs when DM annihilates through a near-resonant mediator. We have shown that, for a DM mass slightly smaller than half the mediator mass, the relic abundance is determined in a model-independent way by the invisible width of the mediator. The cases of Z or Higgs as mediators offer interesting applications to our results. As shown in figure 6, Z and Higgs invisible widths below their experimental limits are compatible with DM thermal abundance and with the LUX constraint. Thus, the search for invisible Higgs decays that can be performed at the LHC and at future facilities (and, possibly, improvements in the measurement of the Z invisible width at GigaZ) offer very interesting ways to probe the nature of the DM.

Acknowledgments

We thank E. del Nobile, P. Panci and A. Urbano for useful discussions. ADS acknowledges partial support from the European Union FP7 ITN INVISIBLES (Marie Curie Actions, PITN-GA-2011-289442). This work was supported by the ESF grant MTT8 and by the SF0690030s09 project and by the European Programme PITN-GA-2009-237920 (UNILHC).

A Colour tensor products

We give here some details about the decomposition of the $\bar{\chi}'_I\chi'_J \to g^a g^b$ scattering rate into two-body channels with given colour. The total scattering amplitude is proportional to $A^{ab}_{IJ} = \{T^a, T^b\}_{IJ}$, for both fermion and scalar particles χ'. Here $(T^a)_{IJ}$ are the colour generators in the desired representation: $(T^a)_{ij} = \lambda^a_{ij}/2$ for triplets and $(T^a)_{bc} = -if^a_{bc}$ for octets.

When χ' is a colour triplet, the rate has to be decomposed into the $3\otimes\bar{3} = 1\oplus 8$ channels. The total amplitude $A^{ab}|^k_i$ can be split into singlet and octet amplitudes according to

$$A^{ab}|^k_i = [\mathbf{1}]^{ab}|^k_i + [\mathbf{8}]^{ab}|^k_i\,, \tag{A.1}$$

$$[\mathbf{1}]^{ab}\,|^k_i = \frac{1}{3}\delta^k_i A^{ab}|^m_m\,, \qquad [\mathbf{8}]^{ab}|^k_i = A^{ab}|^k_i - \frac{1}{3}\delta^k_i A^{ab}|^m_m\,. \tag{A.2}$$

JHEP06(2014)081

When we take the modulus squared of the amplitude in eq. (A.1) and sum over colour indices, the interference terms vanish and we are left with the squares of the individual amplitudes, which are given by

$$\frac{7}{2}\sum_{abik}\left|[\mathbf{1}]^{ab}{}^{k}_{i}\right|^2=\frac{7}{5}\sum_{abik}\left|[\mathbf{8}]^{ab}{}^{k}_{i}\right|^2=\sum_{abik}\left|A^{ab}{}^{k}_{i}\right|^2 . \tag{A.3}$$

This result explains the factors in eq. (2.19).

When χ' is a color octet, the rate has to be decomposed into the $8\otimes 8=1_S\oplus 8_A\oplus 8_S\oplus 10_A\oplus\overline{10}_A\oplus 27_S$ channels. The total amplitude can be written as A^{lk}_{ij}. The pair of fundamental and anti-fundamental indices (i,l), subject to a traceless condition ($A^{mk}_{mj}=0$), describe one octet; the pair of indices (j,k) under the traceless condition ($A^{lm}_{im}=0$) describe the second octet; for the sake of readability, we drop the indices a and b of the final-state gluons. The total amplitude can be decomposed as

$$A^{lk}_{ij}=[\mathbf{1_S}]^{lk}_{ij}+[\mathbf{8_A}]^{lk}_{ij}+[\mathbf{8_S}]^{lk}_{ij}+[\mathbf{10_A}]^{lk}_{ij}+[\overline{\mathbf{10}}_\mathbf{A}]^{lk}_{ij}+[\mathbf{27_S}]^{lk}_{ij}\,, \tag{A.4}$$

$$[\mathbf{1_S}]^{lk}_{ij}=\frac{1}{8}A^{nm}_{mn}\left(\delta^k_i\delta^l_j-\frac{1}{3}\delta^l_i\delta^k_j\right) \tag{A.5}$$

$$[\mathbf{8_A}]^{lk}_{ij}=\frac{1}{6}\left[\delta^l_j(A^{mk}_{im}-A^{km}_{mi})-\delta^k_i(A^{ml}_{jm}-A^{lm}_{mj})\right] \tag{A.6}$$

$$\begin{aligned}[\mathbf{8_S}]^{lk}_{ij}=&\frac{1}{20}\left[\delta^k_i(A^{lm}_{mj}+A^{ml}_{jm})+\delta^k_j(A^{lm}_{mi}+A^{ml}_{im})+\delta^l_i(A^{km}_{mj}+A^{mk}_{jm})+\delta^l_j(A^{km}_{mi}+A^{mk}_{im})\right]+\\&+\frac{1}{4}(A^{lk}_{ij}-A^{lk}_{ji}-A^{kl}_{ij}+A^{kl}_{ji})+\frac{1}{60}(\delta^l_i\delta^k_j-9\delta^k_i\delta^l_j)A^{nm}_{mn}\end{aligned} \tag{A.7}$$

$$\begin{aligned}[\mathbf{10_A}]^{lk}_{ij}=&\frac{1}{4}(A^{lk}_{ij}-A^{lk}_{ji}+A^{kl}_{ij}-A^{kl}_{ji})-\frac{1}{12}\left[\delta^l_j(A^{mk}_{im}-A^{km}_{mi})+\right.\\&\left.-\delta^l_i(A^{mk}_{jm}-A^{km}_{mj})+\delta^k_j(A^{ml}_{im}-A^{lm}_{mi})-\delta^k_i(A^{ml}_{jm}-A^{lm}_{mj})\right]\end{aligned} \tag{A.8}$$

$$\begin{aligned}[\overline{\mathbf{10}}_\mathbf{A}]^{lk}_{ij}=&\frac{1}{4}(A^{lk}_{ij}+A^{lk}_{ji}-A^{kl}_{ij}-A^{kl}_{ji})-\frac{1}{12}\left[\delta^l_j(A^{mk}_{im}-A^{km}_{mi})+\right.\\&\left.+\delta^l_i(A^{mk}_{jm}-A^{km}_{mj})-\delta^k_j(A^{ml}_{im}-A^{lm}_{mi})-\delta^k_i(A^{ml}_{jm}-A^{lm}_{mj})\right]\end{aligned} \tag{A.9}$$

$$\begin{aligned}[\mathbf{27_S}]^{lk}_{ij}=&\frac{1}{4}(A^{lk}_{ij}+A^{lk}_{ji}+A^{kl}_{ij}+A^{kl}_{ji})-\frac{1}{20}[\delta^k_i(A^{lm}_{mj}+A^{ml}_{jm})+\delta^k_j(A^{lm}_{mi}+A^{ml}_{im})+\\&+\delta^l_i(A^{km}_{mj}+A^{mk}_{jm})+\delta^l_j(A^{km}_{mi}+A^{mk}_{im})]+\frac{1}{40}(\delta^l_i\delta^k_j+\delta^k_i\delta^l_j)A^{nm}_{mn}\,.\end{aligned} \tag{A.10}$$

In the modulus squared of the amplitude in eq. (A.4) summed over colour indices, there are no interference terms and the only non-vanishing terms are

$$6\sum|[\mathbf{1_S}]|^2=3\sum|[\mathbf{8_S}]|^2=2\sum|[\mathbf{27_S}]|^2=\sum|A|^2\,. \tag{A.11}$$

This explains the factors in eq. (2.25).

JHEP06(2014)081

References

[1] A. Birkedal, K. Matchev and M. Perelstein, *Dark matter at colliders: A Model independent approach*, *Phys. Rev.* **D 70** (2004) 077701 [hep-ph/0403004] [INSPIRE].

[2] J.L. Feng, S. Su and F. Takayama, *Lower limit on dark matter production at the large hadron collider*, *Phys. Rev. Lett.* **96** (2006) 151802 [hep-ph/0503117] [INSPIRE].

[3] M. Beltrán, D. Hooper, E.W. Kolb and Z.C. Krusberg, *Deducing the nature of dark matter from direct and indirect detection experiments in the absence of collider signatures of new physics*, *Phys. Rev.* **D 80** (2009) 043509 [arXiv:0808.3384] [INSPIRE].

[4] Q.-H. Cao, C.-R. Chen, C.S. Li and H. Zhang, *Effective Dark Matter Model: Relic density, CDMS II, Fermi LAT and LHC*, *JHEP* **08** (2011) 018 [arXiv:0912.4511] [INSPIRE].

[5] M. Beltrán, D. Hooper, E.W. Kolb, Z.A.C. Krusberg and T.M.P. Tait, *Maverick dark matter at colliders*, *JHEP* **09** (2010) 037 [arXiv:1002.4137] [INSPIRE].

[6] P. Agrawal, Z. Chacko, C. Kilic and R.K. Mishra, *A Classification of Dark Matter Candidates with Primarily Spin-Dependent Interactions with Matter*, arXiv:1003.1912 [INSPIRE].

[7] J. Goodman, M. Ibe, A. Rajaraman, W. Shepherd, T.M.P. Tait et al., *Constraints on Light Majorana dark Matter from Colliders*, *Phys. Lett.* **B 695** (2011) 185 [arXiv:1005.1286] [INSPIRE].

[8] Y. Bai, P.J. Fox and R. Harnik, *The Tevatron at the Frontier of Dark Matter Direct Detection*, *JHEP* **12** (2010) 048 [arXiv:1005.3797] [INSPIRE].

[9] J. Fan, M. Reece and L.-T. Wang, *Non-relativistic effective theory of dark matter direct detection*, *JCAP* **11** (2010) 042 [arXiv:1008.1591] [INSPIRE].

[10] J. Goodman, M. Ibe, A. Rajaraman, W. Shepherd, T.M.P. Tait and H.-B. Yu, *Constraints on Dark Matter from Colliders*, *Phys. Rev.* **D 82** (2010) 116010 [arXiv:1008.1783] [INSPIRE].

[11] J. Goodman, M. Ibe, A. Rajaraman, W. Shepherd, T.M.P. Tait and H.-B. Yu, *Gamma Ray Line Constraints on Effective Theories of Dark Matter*, *Nucl. Phys.* **B 844** (2011) 55 [arXiv:1009.0008] [INSPIRE].

[12] K. Cheung, P.-Y. Tseng and T.-C. Yuan, *Cosmic Antiproton Constraints on Effective Interactions of the Dark Matter*, *JCAP* **01** (2011) 004 [arXiv:1011.2310] [INSPIRE].

[13] J.-M. Zheng, Z.-H. Yu, J.-W. Shao, X.-J. Bi, Z. Li et al., *Constraining the interaction strength between dark matter and visible matter: I. fermionic dark matter*, *Nucl. Phys.* **B 854** (2012) 350 [arXiv:1012.2022] [INSPIRE].

[14] P.J. Fox, R. Harnik, J. Kopp and Y. Tsai, *LEP Shines Light on Dark Matter*, *Phys. Rev.* **D 84** (2011) 014028 [arXiv:1103.0240] [INSPIRE].

[15] J.-F. Fortin and T.M.P. Tait, *Collider Constraints on Dipole-Interacting Dark Matter*, *Phys. Rev.* **D 85** (2012) 063506 [arXiv:1103.3289] [INSPIRE].

[16] M.R. Buckley, *Asymmetric Dark Matter and Effective Operators*, *Phys. Rev.* **D 84** (2011) 043510 [arXiv:1104.1429] [INSPIRE].

[17] K. Cheung, P.-Y. Tseng and T.-C. Yuan, *Gamma-ray Constraints on Effective Interactions of the Dark Matter*, *JCAP* **06** (2011) 023 [arXiv:1104.5329] [INSPIRE].

JHEP06(2014)081

[18] J. Wang, C.S. Li, D.Y. Shao and H. Zhang, *Next-to-leading order QCD predictions for the signal of Dark Matter and photon associated production at the LHC*, *Phys. Rev.* **D 84** (2011) 075011 [arXiv:1107.2048] [INSPIRE].

[19] M.T. Frandsen, F. Kahlhoefer, S. Sarkar and K. Schmidt-Hoberg, *Direct detection of dark matter in models with a light Z'*, *JHEP* **09** (2011) 128 [arXiv:1107.2118] [INSPIRE].

[20] A. Rajaraman, W. Shepherd, T.M.P. Tait and A.M. Wijangco, *LHC Bounds on Interactions of Dark Matter*, *Phys. Rev.* **D 84** (2011) 095013 [arXiv:1108.1196] [INSPIRE].

[21] G.F. Giudice, B. Gripaios and R. Mahbubani, *Counting dark matter particles in LHC events*, *Phys. Rev.* **D 85** (2012) 075019 [arXiv:1108.1800] [INSPIRE].

[22] P. Agrawal, S. Blanchet, Z. Chacko and C. Kilic, *Flavored Dark Matter and Its Implications for Direct Detection and Colliders*, *Phys. Rev.* **D 86** (2012) 055002 [arXiv:1109.3516] [INSPIRE].

[23] P.J. Fox, R. Harnik, J. Kopp and Y. Tsai, *Missing Energy Signatures of Dark Matter at the LHC*, *Phys. Rev.* **D 85** (2012) 056011 [arXiv:1109.4398] [INSPIRE].

[24] J. Goodman and W. Shepherd, *LHC Bounds on UV-Complete Models of Dark Matter*, arXiv:1111.2359 [INSPIRE].

[25] K.N. Abazajian, P. Agrawal, Z. Chacko and C. Kilic, *Lower Limits on the Strengths of Gamma Ray Lines from WIMP Dark Matter Annihilation*, *Phys. Rev.* **D 85** (2012) 123543 [arXiv:1111.2835] [INSPIRE].

[26] I.M. Shoemaker and L. Vecchi, *Unitarity and Monojet Bounds on Models for DAMA, CoGeNT and CRESST-II*, *Phys. Rev.* **D 86** (2012) 015023 [arXiv:1112.5457] [INSPIRE].

[27] R. Ding and Y. Liao, *Spin 3/2 Particle as a Dark Matter Candidate: an Effective Field Theory Approach*, *JHEP* **04** (2012) 054 [arXiv:1201.0506] [INSPIRE].

[28] K. Cheung, P.-Y. Tseng, Y.-L.S. Tsai and T.-C. Yuan, *Global Constraints on Effective Dark Matter Interactions: Relic Density, Direct Detection, Indirect Detection and Collider*, *JCAP* **05** (2012) 001 [arXiv:1201.3402] [INSPIRE].

[29] H. An, X. Ji and L.-T. Wang, *Light Dark Matter and Z' Dark Force at Colliders*, *JHEP* **07** (2012) 182 [arXiv:1202.2894] [INSPIRE].

[30] P.J. Fox, R. Harnik, R. Primulando and C.-T. Yu, *Taking a Razor to Dark Matter Parameter Space at the LHC*, *Phys. Rev.* **D 86** (2012) 015010 [arXiv:1203.1662] [INSPIRE].

[31] A.L. Fitzpatrick, W. Haxton, E. Katz, N. Lubbers and Y. Xu, *The Effective Field Theory of Dark Matter Direct Detection*, *JCAP* **02** (2013) 004 [arXiv:1203.3542] [INSPIRE].

[32] M.T. Frandsen, F. Kahlhoefer, A. Preston, S. Sarkar and K. Schmidt-Hoberg, *LHC and Tevatron Bounds on the Dark Matter Direct Detection Cross-Section for Vector Mediators*, *JHEP* **07** (2012) 123 [arXiv:1204.3839] [INSPIRE].

[33] V. Barger, W.-Y. Keung, D. Marfatia and P.-Y. Tseng, *Dipole Moment Dark Matter at the LHC*, *Phys. Lett.* **B 717** (2012) 219 [arXiv:1206.0640] [INSPIRE].

[34] M. Garny, A. Ibarra, M. Pato and S. Vogl, *Closing in on mass-degenerate dark matter scenarios with antiprotons and direct detection*, *JCAP* **11** (2012) 017 [arXiv:1207.1431] [INSPIRE].

[35] M.T. Frandsen, U. Haisch, F. Kahlhoefer, P. Mertsch and K. Schmidt-Hoberg, *Loop-induced dark matter direct detection signals from gamma-ray lines*, *JCAP* **10** (2012) 033 [arXiv:1207.3971] [INSPIRE].

JHEP06(2014)081

[36] Y. Bai and T.M.P. Tait, *Searches with Mono-Leptons*, *Phys. Lett.* **B 723** (2013) 384 [arXiv:1208.4361] [INSPIRE].

[37] U. Haisch, F. Kahlhoefer and J. Unwin, *The impact of heavy-quark loops on LHC dark matter searches*, *JHEP* **07** (2013) 125 [arXiv:1208.4605] [INSPIRE].

[38] N.F. Bell, J.B. Dent, A.J. Galea, T.D. Jacques, L.M. Krauss et al., *Searching for Dark Matter at the LHC with a Mono-Z*, *Phys. Rev.* **D 86** (2012) 096011 [arXiv:1209.0231] [INSPIRE].

[39] F.P. Huang, C.S. Li, J. Wang and D.Y. Shao, *Searching for the signal of dark matter and photon associated production at the LHC beyond leading order*, *Phys. Rev.* **D 87** (2013) 094018 [arXiv:1210.0195] [INSPIRE].

[40] R.C. Cotta, J.L. Hewett, M.P. Le and T.G. Rizzo, *Bounds on Dark Matter Interactions with Electroweak Gauge Bosons*, *Phys. Rev.* **D 88** (2013) 116009 [arXiv:1210.0525] [INSPIRE].

[41] H. An, R. Huo and L.-T. Wang, *Searching for Low Mass Dark Portal at the LHC*, *Phys. Dark Univ.* **2** (2013) 50 [arXiv:1212.2221] [INSPIRE].

[42] L.M. Carpenter, A. Nelson, C. Shimmin, T.M.P. Tait and D. Whiteson, *Collider searches for dark matter in events with a Z boson and missing energy*, *Phys. Rev.* **D 87** (2013) 074005 [arXiv:1212.3352] [INSPIRE].

[43] A. De Simone, A. Monin, A. Thamm and A. Urbano, *On the effective operators for Dark Matter annihilations*, *JCAP* **02** (2013) 039 [arXiv:1301.1486] [INSPIRE].

[44] N. Zhou, D. Berge and D. Whiteson, *Mono-everything: combined limits on dark matter production at colliders from multiple final states*, *Phys. Rev.* **D 87** (2013) 095013 [arXiv:1302.3619] [INSPIRE].

[45] H. Dreiner, D. Schmeier and J. Tattersall, *Contact Interactions Probe Effective Dark Matter Models at the LHC*, *Europhys. Lett.* **102** (2013) 51001 [arXiv:1303.3348] [INSPIRE].

[46] T. Lin, E.W. Kolb and L.-T. Wang, *Probing dark matter couplings to top and bottom quarks at the LHC*, *Phys. Rev.* **D 88** (2013) 063510 [arXiv:1303.6638] [INSPIRE].

[47] H.M. Lee, M. Park and V. Sanz, *Gravity-mediated (or Composite) Dark Matter*, *Eur. Phys. J.* **C 74** (2014) 2715 [arXiv:1306.4107] [INSPIRE].

[48] B. Bellazzini, M. Cliche and P. Tanedo, *Effective theory of self-interacting dark matter*, *Phys. Rev.* **D 88** (2013) 083506 [arXiv:1307.1129] [INSPIRE].

[49] G. Busoni, A. De Simone, E. Morgante and A. Riotto, *On the Validity of the Effective Field Theory for Dark Matter Searches at the LHC*, *Phys. Lett.* **B 728** (2014) 412 [arXiv:1307.2253] [INSPIRE].

[50] Z.-H. Yu, Q.-S. Yan and P.-F. Yin, *Detecting interactions between dark matter and photons at high energy e^+e^- colliders*, *Phys. Rev.* **D 88** (2013) 075015 [arXiv:1307.5740] [INSPIRE].

[51] S. Profumo, W. Shepherd and T. Tait, *Pitfalls of dark matter crossing symmetries*, *Phys. Rev.* **D 88** (2013) 056018 [arXiv:1307.6277] [INSPIRE].

[52] S. Chang, R. Edezhath, J. Hutchinson and M. Luty, *Effective WIMPs*, *Phys. Rev.* **D 89** (2014) 015011 [arXiv:1307.8120] [INSPIRE].

[53] H. An, L.-T. Wang and H. Zhang, *Dark matter with t-channel mediator: a simple step beyond contact interaction*, arXiv:1308.0592 [INSPIRE].

JHEP06(2014)081

[54] Y. Bai and J. Berger, *Fermion Portal Dark Matter*, *JHEP* **11** (2013) 171 [arXiv:1308.0612] [INSPIRE].

[55] A. DiFranzo, K.I. Nagao, A. Rajaraman and T.M.P. Tait, *Simplified Models for Dark Matter Interacting with Quarks*, *JHEP* **11** (2013) 014 [arXiv:1308.2679] [INSPIRE].

[56] A. Alves, S. Profumo and F.S. Queiroz, *The dark Z' portal: direct, indirect and collider searches*, *JHEP* **04** (2014) 063 [arXiv:1312.5281] [INSPIRE].

[57] O. Buchmueller, M.J. Dolan and C. McCabe, *Beyond Effective Field Theory for Dark Matter Searches at the LHC*, *JHEP* **01** (2014) 025 [arXiv:1308.6799] [INSPIRE].

[58] U. Haisch, F. Kahlhoefer and E. Re, *QCD effects in mono-jet searches for dark matter*, *JHEP* **12** (2013) 007 [arXiv:1310.4491] [INSPIRE].

[59] M.A. Fedderke, E.W. Kolb, T. Lin and L.-T. Wang, *Gamma-ray constraints on dark-matter annihilation to electroweak gauge and Higgs bosons*, *JCAP* **01** (2014) 001 [arXiv:1310.6047] [INSPIRE].

[60] C. Cheung and D. Sanford, *Simplified Models of Mixed Dark Matter*, *JCAP* **02** (2014) 011 [arXiv:1311.5896] [INSPIRE].

[61] N.F. Bell, Y. Cai and A.D. Medina, *Co-annihilating Dark Matter: Effective Operator Analysis and Collider Phenomenology*, arXiv:1311.6169 [INSPIRE].

[62] U. Haisch, A. Hibbs and E. Re, *Determining the structure of dark-matter couplings at the LHC*, *Phys. Rev.* **D 89** (2014) 034009 [arXiv:1311.7131] [INSPIRE].

[63] M.B. Krauss, S. Morisi, W. Porod and W. Winter, *Higher Dimensional Effective Operators for Direct Dark Matter Detection*, *JHEP* **02** (2014) 056 [arXiv:1312.0009] [INSPIRE].

[64] G. Busoni, A. De Simone, J. Gramling, E. Morgante and A. Riotto, *On the Validity of the Effective Field Theory for Dark Matter Searches at the LHC, Part II: Complete Analysis for the s-channel*, arXiv:1402.1275 [INSPIRE].

[65] C.P. Burgess, M. Pospelov and T. ter Veldhuis, *The Minimal model of nonbaryonic dark matter: A Singlet scalar*, *Nucl. Phys.* **B 619** (2001) 709 [hep-ph/0011335] [INSPIRE].

[66] H. Davoudiasl, R. Kitano, T. Li and H. Murayama, *The New minimal standard model*, *Phys. Lett.* **B 609** (2005) 117 [hep-ph/0405097] [INSPIRE].

[67] B. Patt and F. Wilczek, *Higgs-field portal into hidden sectors*, hep-ph/0605188 [INSPIRE].

[68] S. Andreas, T. Hambye and M.H.G. Tytgat, *WIMP dark matter, Higgs exchange and DAMA*, *JCAP* **10** (2008) 034 [arXiv:0808.0255] [INSPIRE].

[69] V. Barger, P. Langacker, M. McCaskey, M. Ramsey-Musolf and G. Shaughnessy, *Complex Singlet Extension of the Standard Model*, *Phys. Rev.* **D 79** (2009) 015018 [arXiv:0811.0393] [INSPIRE].

[70] R.N. Lerner and J. McDonald, *Gauge singlet scalar as inflaton and thermal relic dark matter*, *Phys. Rev.* **D 80** (2009) 123507 [arXiv:0909.0520] [INSPIRE].

[71] X.-G. He, T. Li, X.-Q. Li, J. Tandean and H.-C. Tsai, *The Simplest Dark-Matter Model, CDMS II Results and Higgs Detection at LHC*, *Phys. Lett.* **B 688** (2010) 332 [arXiv:0912.4722] [INSPIRE].

[72] S. Kanemura, S. Matsumoto, T. Nabeshima and N. Okada, *Can WIMP Dark Matter overcome the Nightmare Scenario?*, *Phys. Rev.* **D 82** (2010) 055026 [arXiv:1005.5651] [INSPIRE].

JHEP06(2014)081

[73] V. Barger, Y. Gao, M. McCaskey and G. Shaughnessy, *Light Higgs Boson, Light Dark Matter and Gamma Rays*, *Phys. Rev.* **D 82** (2010) 095011 [arXiv:1008.1796] [INSPIRE].

[74] A. Biswas and D. Majumdar, *The Real Gauge Singlet Scalar Extension of Standard Model: A Possible Candidate of Cold Dark Matter*, *Pramana* **80** (2013) 539 [arXiv:1102.3024] [INSPIRE].

[75] C. Englert, T. Plehn, D. Zerwas and P.M. Zerwas, *Exploring the Higgs portal*, *Phys. Lett.* **B 703** (2011) 298 [arXiv:1106.3097] [INSPIRE].

[76] Y. Mambrini, *Higgs searches and singlet scalar dark matter: Combined constraints from XENON 100 and the LHC*, *Phys. Rev.* **D 84** (2011) 115017 [arXiv:1108.0671] [INSPIRE].

[77] M. Pospelov and A. Ritz, *Higgs decays to dark matter: beyond the minimal model*, *Phys. Rev.* **D 84** (2011) 113001 [arXiv:1109.4872] [INSPIRE].

[78] I. Low, P. Schwaller, G. Shaughnessy and C.E.M. Wagner, *The dark side of the Higgs boson*, *Phys. Rev.* **D 85** (2012) 015009 [arXiv:1110.4405] [INSPIRE].

[79] O. Lebedev, H.M. Lee and Y. Mambrini, *Vector Higgs-portal dark matter and the invisible Higgs*, *Phys. Lett.* **B 707** (2012) 570 [arXiv:1111.4482] [INSPIRE].

[80] A. Djouadi, O. Lebedev, Y. Mambrini and J. Quevillon, *Implications of LHC searches for Higgs-portal dark matter*, *Phys. Lett.* **B 709** (2012) 65 [arXiv:1112.3299] [INSPIRE].

[81] J.F. Kamenik and C. Smith, *Could a light Higgs boson illuminate the dark sector?*, *Phys. Rev.* **D 85** (2012) 093017 [arXiv:1201.4814] [INSPIRE].

[82] L. Lopez-Honorez, T. Schwetz and J. Zupan, *Higgs portal, fermionic dark matter and a Standard Model like Higgs at 125 GeV*, *Phys. Lett.* **B 716** (2012) 179 [arXiv:1203.2064] [INSPIRE].

[83] A. Djouadi, A. Falkowski, Y. Mambrini and J. Quevillon, *Direct Detection of Higgs-Portal Dark Matter at the LHC*, *Eur. Phys. J.* **C 73** (2013) 2455 [arXiv:1205.3169] [INSPIRE].

[84] A. Greljo, J. Julio, J.F. Kamenik, C. Smith and J. Zupan, *Constraining Higgs mediated dark matter interactions*, *JHEP* **11** (2013) 190 [arXiv:1309.3561] [INSPIRE].

[85] A.A. Petrov and W. Shepherd, *Searching for dark matter at LHC with Mono-Higgs production*, *Phys. Lett.* **B 730** (2014) 178 [arXiv:1311.1511] [INSPIRE].

[86] L. Carpenter, A. DiFranzo, M. Mulhearn, C. Shimmin, S. Tulin et al., *Mono-Higgs: a new collider probe of dark matter*, *Phys. Rev.* **D 89** (2014) 075017 [arXiv:1312.2592] [INSPIRE].

[87] G. Arcadi, Y. Mambrini, M.H.G. Tytgat and B. Zaldivar, *Invisible Z' and dark matter: LHC vs LUX constraints*, *JHEP* **03** (2014) 134 [arXiv:1401.0221] [INSPIRE].

[88] A. Crivellin, F. D'Eramo and M. Procura, *New Constraints on Dark Matter Effective Theories from Standard Model Loops*, *Phys. Rev. Lett.* **112** (2014) 191304 [arXiv:1402.1173] [INSPIRE].

[89] M. Cirelli, N. Fornengo and A. Strumia, *Minimal dark matter*, *Nucl. Phys.* **B 753** (2006) 178 [hep-ph/0512090] [INSPIRE].

[90] A. Sommerfeld, *Über die Beugung und Bremsung der Elektronen*, *Ann. Phys.* **11** (1931) 257.

[91] H. Baer, K.-m. Cheung and J.F. Gunion, *A Heavy gluino as the lightest supersymmetric particle*, *Phys. Rev.* **D 59** (1999) 075002 [hep-ph/9806361] [INSPIRE].

JHEP06(2014)081

[92] J. Hisano, S. Matsumoto and M.M. Nojiri, *Explosive dark matter annihilation*, *Phys. Rev. Lett.* **92** (2004) 031303 [hep-ph/0307216] [INSPIRE].

[93] J. Hisano, S. Matsumoto, M.M. Nojiri and O. Saito, *Non-perturbative effect on dark matter annihilation and gamma ray signature from galactic center*, *Phys. Rev.* **D 71** (2005) 063528 [hep-ph/0412403] [INSPIRE].

[94] A. Strumia, *Sommerfeld corrections to type-II and III leptogenesis*, *Nucl. Phys.* **B 809** (2009) 308 [arXiv:0806.1630] [INSPIRE].

[95] N. Arkani-Hamed, D.P. Finkbeiner, T.R. Slatyer and N. Weiner, *A Theory of Dark Matter*, *Phys. Rev.* **D 79** (2009) 015014 [arXiv:0810.0713] [INSPIRE].

[96] J.L. Feng, M. Kaplinghat and H.-B. Yu, *Sommerfeld Enhancements for Thermal Relic Dark Matter*, *Phys. Rev.* **D 82** (2010) 083525 [arXiv:1005.4678] [INSPIRE].

[97] A. Freitas, *Radiative corrections to co-annihilation processes*, *Phys. Lett.* **B 652** (2007) 280 [arXiv:0705.4027] [INSPIRE].

[98] A. Hryczuk, *The Sommerfeld enhancement for scalar particles and application to sfermion co-annihilation regions*, *Phys. Lett.* **B 699** (2011) 271 [arXiv:1102.4295] [INSPIRE].

[99] W. Fischler, *Quark - anti-Quark Potential in QCD*, *Nucl. Phys.* **B 129** (1977) 157.

[100] Y. Schröder, *The Static potential in QCD to two loops*, *Phys. Lett.* **B 447** (1999) 321 [hep-ph/9812205] [INSPIRE].

[101] A. Delgado, G.F. Giudice, G. Isidori, M. Pierini and A. Strumia, *The light stop window*, *Eur. Phys. J.* **C 73** (2013) 2370 [arXiv:1212.6847] [INSPIRE].

[102] J. Alwall, M. Herquet, F. Maltoni, O. Mattelaer and T. Stelzer, *MadGraph 5 : Going Beyond*, *JHEP* **06** (2011) 128 [arXiv:1106.0522] [INSPIRE].

[103] ATLAS collaboration, *Search for New Phenomena in Monojet plus Missing Transverse Momentum Final States using 10 fb^{-1} of pp Collisions at $\sqrt{s} = 8$ TeV with the ATLAS detector at the LHC*, ATLAS-CONF-2012-147 (2012).

[104] CMS collaboration, *Search for new physics in monojet events in pp collisions at $\sqrt{s}$= 8 TeV*, CMS-PAS-EXO-12-048.

[105] L.T. Wang, talk at BSM Opportunities at 100 TeV, CERN (2014), https://indico.cern.ch/event/284800/session/0/contribution/5/material/slides/0.pdf.

[106] M. Cirelli, E. Del Nobile and P. Panci, *Tools for model-independent bounds in direct dark matter searches*, *JCAP* **10** (2013) 019 [arXiv:1307.5955] [INSPIRE].

[107] LUX collaboration, D.S. Akerib et al., *First results from the LUX dark matter experiment at the Sanford Underground Research Facility*, *Phys. Rev. Lett.* **112** (2014) 091303 [arXiv:1310.8214] [INSPIRE].

[108] U. Haisch and F. Kahlhoefer, *On the importance of loop-induced spin-independent interactions for dark matter direct detection*, *JCAP* **04** (2013) 050 [arXiv:1302.4454] [INSPIRE].

[109] G.F. Giudice, A. Notari, M. Raidal, A. Riotto and A. Strumia, *Towards a complete theory of thermal leptogenesis in the SM and MSSM*, *Nucl. Phys.* **B 685** (2004) 89 [hep-ph/0310123] [INSPIRE].

JHEP06(2014)081